International Journal of
Molecular Sciences

MDPI

Article

MicroRNA Profiling in Serum Reveals Host–Virus Interactions Associated with Epstein–Barr Virus in Persons with Multiple Sclerosis

Dusadee Ospondpant [1], Na Zhang [2], Umama Z. Siddiqi [1], William G. Branton [1], Hajar Miranzadeh Mahabadi [1], Eric A. Cohen [3,4], Nabeela Nathoo [1], Pam Dumont [1], Jason Plemel [1], Penelope Smyth [1], Linglong Kong [2], Carlos Camara-Lemarroy [5] and Christopher Power [1,6,7,*]

[1] Departments of Medicine, University of Alberta, Edmonton, AB T6G 2R3, Canada
[2] Mathematical & Statistical Sciences, University of Alberta, Edmonton, AB T6G 2R3, Canada
[3] Institut de Recherches Cliniques de Montréal (IRCM), Montreal, QC H3C 3J7, Canada
[4] Department of Microbiology, Infectiology & Immunology, Université de Montréal, Montreal, QC H3C 3J7, Canada
[5] Department of Clinical Neurosciences, University of Calgary, Calgary, AB T2N 1N4, Canada
[6] Medical Microbiology & Immunology, University of Alberta, Edmonton, AB T6G 2R3, Canada
[7] Li Ka Shing Institute of Virology, 6-11 Heritage Medical Research Centre, University of Alberta, Edmonton, AB T6N 2S6, Canada
* Correspondence: chris.power@ualberta.ca; Tel.:+780-407-1938

Abstract

Multiple sclerosis (MS) is a chronic immune-mediated neurological disorder that affects 2.9 million persons globally; however, the disease course and the underlying pathogenic determinants remain uncertain. Epstein–Barr virus (EBV) is a proposed etiologic cofactor for MS despite its ubiquity in most human populations. This study investigated viral- and host-encoded miRNAs in serum from persons with (PwMS) or without (PwoMS) MS with the goal of identifying miRNAs associated with MS phenotypes and responses to therapy. PwMS (n = 80) were stratified by low and high Expanded Disability Status Scale (EDSS) scores or B-cell depletion therapy (BCDT) status and compared to PwoMS (n = 39) in Discovery (DC) and Validation (VC) Cohorts. miRNAs were measured by sequencing in the DC and verified by droplet digital PCR (ddPCR) in the VC. EBV viremia (*EBNA1* and *EBER1* DNA copies/mL) was measured by ddPCR. Machine-learning analyses prioritized candidate miRNAs for further evaluation. Here, hsa-miR-26b-5p was suppressed in High-EDSS PwMS (n = 40) (DC: read-difference = −733.4; VC: copy-difference = 3160; $p < 0.05$) while hsa-miR-181d-5p was suppressed in the Low-EDSS PwMS (n = 40) (DC: read-difference = 17.1; VC: copy-difference = 38.9; $p < 0.05$), compared to PwoMS. In both the DC and VC, EBV-*EBNA1* correlated with EBV-*EBER1* levels ($\varrho = 0.6$, $p < 0.05$) and age ($\varrho = 0.3$, $p < 0.05$). ebv-miR-BART11-5p, identified in the DC by sequencing, was increased in Low-EDSS versus High-EDSS PwMS in the VC (copy-difference = 22.5, $p < 0.05$). In PwMS without BCDT versus PwoMS, hsa-miR-26b-5p was decreased in both cohorts (DC: read-difference = 778.9; VC: copy-difference = 727; $p < 0.05$). ebv-miR-BART11-5p levels correlated with both *EBNA1* and *EBER1* levels among PwMS without BCDT ($r^2 = 0.3$, $p < 0.05$). In conclusion, this study identified previously unrecognized miRNAs, hsa-miR-181d-5p, hsa-miR-26b-5p, and ebv-miR-BART11-5p, associated with EBV viremia, BCDT, and disease severity in PwMS. These findings highlight multiple host–virus molecular interactions in MS across the Discovery and Validation Cohorts.

Keywords: multiple sclerosis; Epstein–Barr virus; microRNAs; B-cell depletion therapy; serum biomarkers

Check for updates

Academic Editor: Monique F. Stins

Received: 3 October 2026
Revised: 18 November 2026
Accepted: 21 November 2026
Published: 24 November 2026

Copyright: © 2026 by the authors. Licensee MDPI, Basel, Switzerland. This article is an open access article distributed under the terms and conditions of the Creative Commons Attribution (CC BY) license.

1. Introduction

Multiple sclerosis (MS) is a chronic immune-mediated demyelinating disease of the central nervous system (CNS) with onset typically between the ages of 20–40 years, that affects 2.9 million persons globally [1]. Moreover, the MS disease course and response to therapies remain unclear. Although the etiology of MS is uncertain, several factors such as immune dysregulation, genetic susceptibility, and environmental factors contribute to neuroinflammation, demyelination, and neurodegeneration, leading to progressive neurological disability in MS [2].

Among environmental factors, Epstein–Barr virus (EBV) has emerged as one of the most debated candidate triggers for MS. EBV is a human gammaherpesvirus that infects approximately 95% of the global adult population and shows a high prevalence among persons with MS [3,4]. A large longitudinal study of U.S. military personnel demonstrated that the risk of MS increased 32-fold following EBV infection [3]. As a putative etiological agent, EBV establishes lifelong infection in B cells and has been detected within MS brain lesions [4]. B cells are the primary reservoir for latent EBV, and B-cell depletion therapies (BCDTs), such as anti-CD20 antibodies, are recognized as effective therapies for autoimmune diseases like MS. This treatment might reduce EBV-infected B cells and EBV-associated inflammation [5,6]. Together, these findings suggest that EBV infection might represent a disease cofactor in MS, although the exact mechanisms remain unknown.

Diagnosing MS remains a challenge because of the disease's clinical heterogeneity. Additionally, the frequency, duration, and evolution of symptoms and signs in the same person with MS over time complicate diagnosis and therapy selection [7]. The diagnosis of MS is currently based on clinical assessment and investigations, including MRI and CSF analyses [8]. As there is no single accurate and reliable diagnostic test for MS, a molecular biomarker is an imperative need to support diagnosis and treatment. MicroRNAs (miRNAs) are small RNAs encoded by viral and host genomes that modulate the expression and function of viral and cellular transcripts and proteins [9]. Circulating miRNAs are promising non-invasive biomarkers due to their remarkable stability in extracellular fluids. Dysregulated miRNA expression profiles can serve as indicators of disease, including cancer and neurological disorders, and offer insights into pathogenesis, diagnosis, and therapy [10].

Given that EBV infection is a proposed risk factor for MS, yet its disease course, pathogenesis, and variable responses to current therapies remain uncertain, prior studies of circulating miRNAs in MS have mainly focused on host-encoded miRNAs in peripheral blood mononuclear cells (PBMCs) or plasma, rarely examining EBV-encoded miRNAs or stratifying by disease severity or treatment. Therefore, this study aimed to determine miRNAs encoded by both EBV and host in serum from PwMS, stratified by disease severity and BCDT status, compared with persons without MS (PwoMS). This study design enabled analyses of virus- and host-encoded miRNAs, together across disease severity and treatment status, and revealed exploratory correlations between EBV- and host-encoded miRNAs with disease severity and treatment response.

2. Results

2.1. Clinical Cohorts

Among 119 participants in the Discovery Cohort (DC; n = 48) and Validation Cohort (VC; n = 71), persons with (PwMS) and without MS (PwoMS) were matched for sex and age (mean[SD]): the DC included PwoMS (50% female, 41.4[9.6]), Low-Expanded Disability Status Scale (EDSS) PwMS (56% female, 43.4[8.9]), High-EDSS PwMS (56% female, 41.7[8.7]); the VC included PwoMS (78% female, 43.0[9.5]), Low-EDSS PwMS (71% female, 42.0[9.8]), High-EDSS PwMS (71% female, 43.1[9.8]) (Table 1; Figure 1). PwMS were stratified into low- and high-disability groups based on EDSS scores, ranging from 0–2.5 (low disability) and 3–6.5

(high disability) groups ($p < 0.001$). The modified fatigue impact scale (MFIS) is a patient-reported measure of fatigue in which higher total and subscale scores (physical, cognitive, and psychosocial) indicate greater fatigue-related disability and therefore a worsened patient status. In this study, total MFIS scores and all subscale scores were significantly increased in PwMS compared to PwoMS in the High-EDSS group in both cohorts (Table 1; all $p < 0.05$). In the Low-EDSS group, the MFIS score did not differ significantly from PwoMS in the DC, whereas significant increases were observed in the VC (all $p < 0.05$). Within the PwMS group, the High-EDSS group showed higher MFIS scores across all scales compared to the Low-EDSS group for both cohorts ($p < 0.05$).

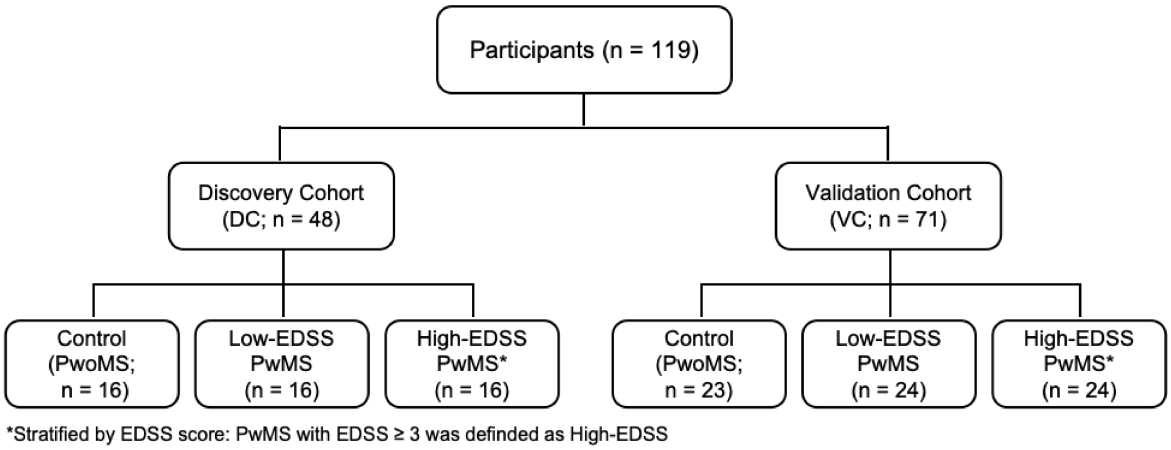

Figure 1. Flow diagram delineating PwoMS and PwMS with disease-severity stratification and the number of participants in the Discovery and Validation Cohorts.

2.2. Host-Encoded miRNAs Associated with Disease Severity in PwMS

Over 1000 host-encoded miRNAs were detected in sera from the DC. A multivariate machine-learning model identified the top 18 miRNAs with variable importance scores of greater than 75% (Figure 2A). The levels of six host-encoded miRNAs, including miR-10a-5p, miR-10b-5p, miR-26b-5p, miR-181d-5p, miR-499a-5p, and miR-4435, were significantly different between PwMS (Low- or High-EDSS) and PwoMS in the DC (Figure 2B,C and Supplementary Figure S1A). ROC curve analysis of these miRNAs revealed an AUROC greater than 0.7 ($p < 0.05$; Supplementary Figure S1B), indicating robust discrimination of PwMS (Low- or High-EDSS) from PwoMS. Comparison of the DC and VC revealed that hsa-miR-26b-5p (Figure 2B; read difference = −733.4, 95%CI = −1143 to −185, $p = 0.01$, $q = 0.03$) and hsa-miR-181d-5p (Figure 2C; read difference = 17.1, 95%CI = 4.5–29.6, $p = 0.005$, $q = 0.002$) levels were significantly decreased in the High-EDSS and Low-EDSS PwMS, respectively, compared to PwoMS in the DC. Similarly, mean hsa-miR-26b-5p (Figure 2D; copy difference = 3160, 95%CI = 107–6213, $p = 0.04$, $q < 0.05$) and hsa-miR-181d-5p levels (Figure 2F; copy difference = 38.9, 95%CI = 1.2–76.6, $p < 0.05$, $q = 0.03$) were significantly decreased in the High-EDSS and Low-EDSS PwMS, respectively, compared to PwoMS in the VC. However, the discriminatory performance of these host miRNAs in the VC was modest (AUROC 0.62–0.66, $p > 0.05$; Supplementary Figure S1C), indicating that these are candidate rather than clinically valid biomarkers. Given the consistent findings between the two cohorts using different detection methods (miRNA sequencing and ddPCR), we examined the expression of host gene proteins targeted by these two miRNAs using a proteomics database of cerebral white matter from PwMS and PwoMS [11]. TarBase-predicted targets for hsa-miR-26b-5p (382 targets) and hsa-miR-181d-5p (412 targets) were intersected with proteins significantly upregulated in white matter from PwMS compared to PwoMS. The proteins shown in Figure 2E,G are predicted targets detected as significantly upregulated in this dataset [11], with no further selection based

on miRNA-protein correlation. Functional annotation of these proteins indicated that they are associated with metabolic (e.g., MAT2A and NAMPT) and NOD-like receptor signaling (e.g., NEK7) functions. These findings verified previous reports of the association between hsa-miR-26b-5p and MS, while also advancing the discovery of a novel miRNA (hsa-miR-181d-5p) associated with MS based on different techniques and highlighting differential expression in the brain of proteins targeted by these miRNAs.

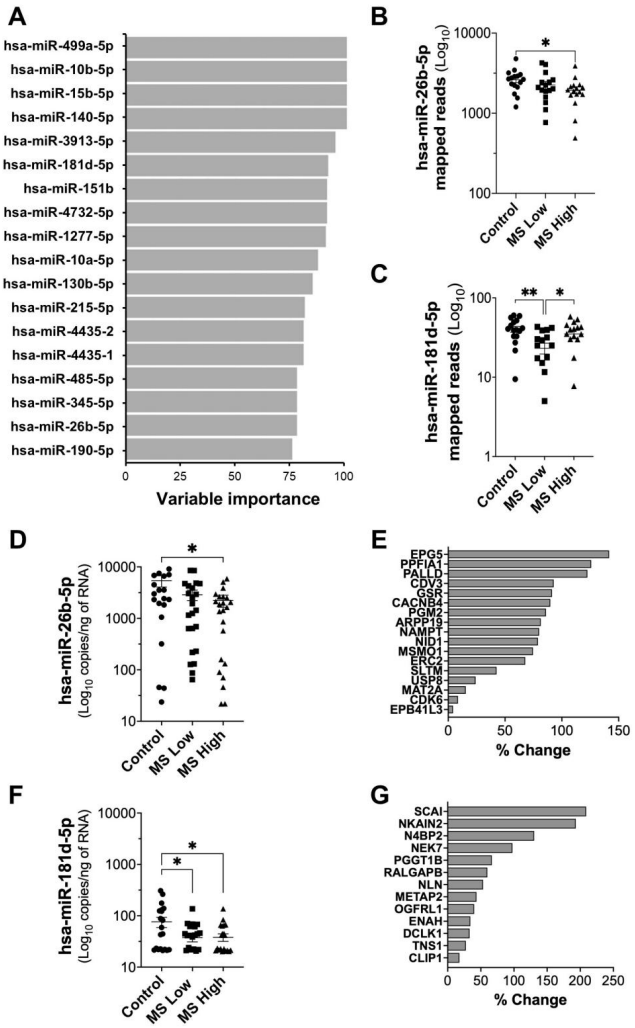

Figure 2. Differential expression of serum host-encoded miRNAs and their targets in persons with MS with low and high disability. (**A**–**C**) In the Discovery Cohort. (**A**) Variable importance scores from a multivariate machine-learning model, identifying the top 18 host-encoded miRNAs. Differential expression of identified host-encoded miRNAs (**B**) hsa-miR-26b-5p; Mann–Whitney *U* test showed a significant difference between the control and High-EDSS PwMS (U = 61, $p = 0.01$), and (**C**) hsa-miR-181d-5p; one-way ANOVA with Tukey's post hoc test showed a significant difference among groups ($F(2,45) = 5$, $p = 0.005$) was measured using miRNA sequencing. (**D**,**F**) In the Validation Cohort. Serum levels of (**D**) hsa-miR-26b-5p; one-way ANOVA with Tukey's post hoc test ($F(2,67) = 3.4$, $p = 0.04$), and (**F**) hsa-miR-181d-5p; one-way ANOVA with Tukey's post hoc test ($F(2,68) = 4.0$, $p = 0.02$) were quantified using ddPCR. (**E**,**G**) Proteomic analysis revealed significant percent increases in cerebral white matter from PwMS compared to PwoMS. Decreased levels of (**E**) hsa-miR-26b-5p and (**G**) hsa-miR-181d-5p were associated with increased host-encoded targeted proteins in cerebral white matter from PwMS. Data are presented as mean ± SEM; * $p < 0.05$, ** $p < 0.01$ for comparison between the control and Low-EDSS or High-EDSS PwMS.

Table 1. Clinical and demographic features of persons with (PwMS) and without MS (PwoMS) in the Discovery and Validation Cohorts.

Clinical Parameters	Discovery Cohort (DC)				Validation Cohort (VC)			
	PwoMS (n = 16)	**Low-EDSS PwMS (n = 16)**	**High-EDSS PwMS (n = 16)**	***p*-Values**	**PwoMS (n = 23)**	**Low-EDSS PwMS (n = 24)**	**High-EDSS PwMS (n = 24)**	***p*-Values**
Sex								
Female (n, %)	8 (50.0%)	9 (56.2%)	9 (56.2%)	>0.5	18 (78.3%)	17 (70.8%)	17 (70.8%)	>0.5
Male (n, %)	8 (50.0%)	7 (43.8%)	7 (43.8%)	>0.5	5 (21.7%)	7 (29.2%)	7 (29.2%)	>0.5
Age								
Mean ± SD (years)	41.4 ± 9.6	43.4 ± 8.9	41.7 ± 8.7	>0.5	43.0 ± 9.5	42.0 ± 9.8	43.1 ± 9.8	>0.5
Range (years)	29–55	30–56	30–55		23–59	23–58	23–59	
EDSS								
Mean ± SD	NA	0.9 ± 0.8	3.7 ± 1.1	<0.001	NA	1.5 ± 1.0	3.7 ± 0.7	<0.001
Range	NA	0–2.5	3–6.5		NA	0–2.5	3–6.5	
Disease duration (years)	NA	7.3 ± 4.6	8.3 ± 4.7	0.47	NA	7.7 ± 4.3	9.1 ± 4.7	0.29
MFIS (Mean ± SD; n)								
Total scale	22.0 ± 21.2; 16	22.0 ± 16.7; 16	45.8 ± 17.9; 16	<0.01	18.3 ± 15.8; 23	40.0 ± 19.8; 19	50.2 ± 18.3; 17	<0.001
Physical scale	8.7 ± 9.4; 16	8.8 ± 7.9; 16	21.6 ± 6.7; 16	<0.001	6.9 ± 7.2; 23	17.5 ± 8.9; 19	23.9 ± 8.9; 17	<0.001
Cognitive scale	11.5 ± 10.3; 16	10.9 ± 7.5; 16	20.1 ± 10.1; 16	<0.05	10.1 ± 8.0; 23	18.4 ± 9.5; 19	21.5 ± 9.7; 17	<0.05
Psychosocial scale	1.9 ± 2.3; 16	2.4 ± 2.4; 16	4.1 ± 2.1; 16	<0.05	1.4 ± 1.6; 23	4.1 ± 2.5; 19	4.9 ± 2.4; 17	<0.001
Treatment *								
BCDT (n)	NA	6	1		NA	13	15	
Non-BCDT (n)	NA	10	15		NA	11	9	

Abbreviations: BCDT: B-cell depletion therapy; EDSS: Expanded Disability Status Scale; MS: multiple sclerosis; MFIS: Modified Fatigue Impact Scale; n: number of samples; NA: not applicable. * PwMS (DC, n = 7 and VC, n = 3) were not receiving disease-modifying therapies at the time of enrollment.

2.3. EBV-Encoded miRNAs and DNA Levels

MicroRNA sequencing of serum samples from the DC detected EBV-encoded ebv-miR-BART1-5p and ebv-miR-BART11-5p in three participants. To extend this latter finding, the levels of additional EBV-encoded miRNAs were assessed by ddPCR in the VC, including miRNAs recognized for their involvement in regulating lytic viral activity [12–14] and prior detection in plasma exosomes and whole blood from MS patients [15]. Five EBV-encoded miRNAs were consistently detected in the VC in PwMS and PwoMS (Figures 3A and S2A). Among these miRNAs, mean ebv-miR-BART11-5p levels were increased in Low-EDSS compared to High-EDSS PwMS (Figure 3A; copy difference = 22.5, 95%CI = 0.9–44.1; $p < 0.05$, $q < 0.05$). The discriminatory performance of ebv-miR-BART11-5p between Low- and High-EDSS was modest (AUROC 0.67, $p = 0.06$; Supplementary Figure S2B). TarBase-predicted targets for ebv-miR-BART11-5p (116 targets) were intersected with host-encoded proteins significantly downregulated in cerebral white matter from PwMS compared to PwoMS (Figure 3B), with a predominance of targeted mitochondrial proteins (e.g., ATP5F1B, MT-CO1, and MT-CO2, and COX7B). The proteins shown represent all predicted targets that met this pre-defined significance criterion, with no further selection based on miRNA-protein correlation. Fatigue is a common symptom in both EBV infection and MS [16–18], and the MFIS is a patient-reported measure in which higher scores indicate greater fatigue-related disability. Therefore, the relationships between EBV-encoded viral miRNAs and MFIS scores were investigated. In the VC, exploratory correlational analyses of EBV-encoded miRNAs with fatigue measurements revealed that ebv-miR-BART20-5p levels were negatively associated with MFIS ($r^2 = 0.6$, 95%CI = −0.9 to −0.2; $p < 0.05$, $q < 0.05$; n = 10; Figure 3C), indicating that lower ebv-miR-BART20-5p levels accompanied with higher fatigue. Likewise, ebv-miR-BART1-5p levels were positively associated with MFIS, in Low-EDSS PwMS ($r^2 = 0.8$, 95%CI = 0.04–0.3; $p < 0.05$, $q < 0.05$; n = 6; Figure 3D), indicating that higher ebv-miR-BART1-5p levels accompanied with higher fatigue. Levels of ebv-miR-BART2-5p increased with age in Low-EDSS PwMS ($r^2 = 0.5$, 95%CI = 0.04–0.2; $p < 0.05$, $q < 0.05$; n = 13; Supplementary Figure S2C, Table 2), while its levels also correlated positively with disease duration in the PwMS Low-EDSS group ($r^2 = 0.3$, 95%CI = 0.01–0.4; $p < 0.05$, $q < 0.05$; n = 13; Supplementary Figure S2D). Mean EBV-encoded *EBNA1* and *EBER1* DNA levels in sera were closely correlated in both the DC ($\varrho = 0.6$; 95%CI = 0.3–0.8; $p < 0.05$, $q < 0.05$; n = 45) and VC ($\varrho = 0.6$; 95%CI = 0.4–0.8; $p < 0.05$, $q < 0.05$; n = 56; Table 2), but were similar across groups (Figure 3E,F). Additionally, *EBNA1* levels were positively correlated with age in both cohorts (DC: $\varrho = 0.3$; 95%CI = 0.05–0.6; $p < 0.05$, $q < 0.05$; n = 43, and VC: $\varrho = 0.3$; 95%CI = 0.01–0.5; $p < 0.05$, $q < 0.05$; n = 57, Table 2). Among Low-EDSS PwMS, combining the DC and VC, *EBNA1* levels were positively correlated with age (Supplementary Figure S2E; $r^2 = 0.2$, 95%CI = 0.03–0.2; $p < 0.05$, $q < 0.05$; n = 36) and negatively correlated with MFIS (Supplementary Figure S2F; $r^2 = 0.2$, 95%CI = −0.8 to −0.06; $p < 0.05$; n = 29). While there were no significant correlations between EBV-encoded miRNAs and DNA levels in the VC across groups, *EBNA1* levels were correlated with ebv-miR-BART20-5p in High-EDSS PwMS ($\varrho = 0.8$; 95%CI = 0.06–1.0; $p = 0.03$, $q < 0.05$; n = 7) and with ebv-miR-BHRF1-3 in Low-EDSS PwMS ($\varrho = 0.8$; 95%CI = 0.2–1.0; $p = 0.03$, $q < 0.05$; n = 8). These data highlighted the expression of serum EBV-encoded miRNAs and their differential expression depending on specific demographic, clinical, and viral genome variables, especially among the Low-EDSS PwMS group. Additionally, analysis within the VC of EBV- and host-encoded miRNAs showed that levels of ebv-miR-BART20-5p were negatively correlated with hsa-miR-26b-5p (Table 2; $\varrho = -0.5$, 95%CI = −0.68 to −0.18; $p < 0.01$, $q < 0.05$; n = 42).

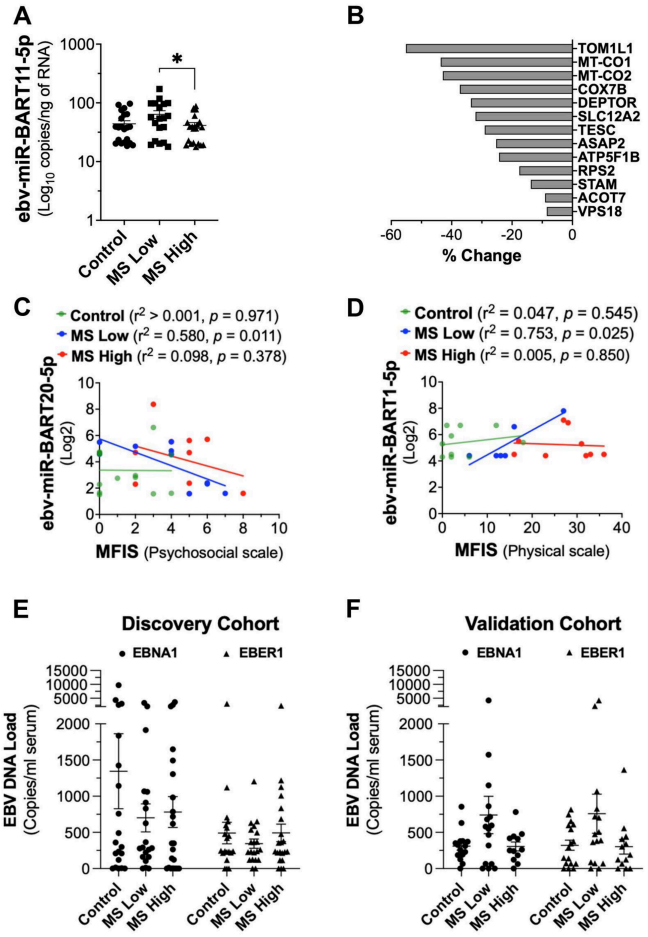

Figure 3. Serum EBV-encoded miRNAs and EBV DNA quantities. (**A**) In the Validation Cohort, ebv-miR-BART11-5p levels were quantified using ddPCR: one-way ANOVA with Tukey's post hoc test showed a significant difference among groups ($F(2,59) = 3.2$, $p = 0.046$) and * $p = 0.04$ for comparison between Low-EDSS and High-EDSS PwMS. (**B**) Proteomic analysis disclosed a significant percentage suppression in cerebral white matter from PwMS compared to PwoMS. Increased level of ebv-miR-BART11-5p was associated with decreased host-encoded proteins in cerebral white matter from PwMS. (**C**,**D**) Linear regression (r^2) analysis showing correlations between EBV-encoded miRNAs and MFIS in PwMS (Low-EDSS, $p < 0.05$) and PwoMS: (**C**) ebv-miR-BART20-5p and MFIS psychosocial, and (**D**) ebv-miR-BART1-5p and physical subscores. (**E**,**F**) EBV DNA (*EBNA1* and *EBER1*) copy numbers were measured in serum from PwMS and PwoMS in the (**E**) Discovery and (**F**) Validation Cohorts. Data are presented as absolute values (mean ± SEM).

Table 2. Exploratory Spearman's correlation coefficients (ϱ) of miRNAs, viral load, and clinical variables in the Validation Cohort.

Variables	Positive Correlation	Negative Correlation
Clinical demographics		
Age	EBNA1 ($\varrho = 0.29$, $p = 0.030$; n = 57)	hsa-miR-10a-5p ($\varrho = -0.25$, $p = 0.035$; n = 71)
	ebv-miR-BART2-5p ($\varrho = 0.45$, $p = 0.004$; n = 39)	hsa-miR-10b-5p ($\varrho = -0.36$, $p = 0.002$; n = 71)
	ebv-miR-BHRF1-3 ($\varrho = 0.52$, $p = 0.01$; n = 24)	hsa-miR-22-5p ($\varrho = -0.29$, $p = 0.014$; n = 71)
		hsa-miR-26b-5p ($\varrho = -0.25$, $p = 0.038$; n = 71)
		hsa-miR-181d-5p ($\varrho = -0.24$, $p = 0.046$; n = 71)
		hsa-miR-192-5p ($\varrho = -0.31$, $p = 0.010$; n = 71)
		hsa-miR-200b-5p ($\varrho = -0.35$, $p = 0.002$; n = 71)

Table 2. *Cont.*

Variables	Positive Correlation	Negative Correlation
		hsa-miR-532-5p ($\varrho = -0.32$, $p = 0.007$; n = 71)
		hsa-let-7i-5p ($\varrho = -0.27$, $p = 0.023$; n = 71)
Disease duration	EBNA1 ($\varrho = 0.43$, $p < 0.001$; n = 38)	
EBER1	EBNA1 ($\varrho = 0.49$, $p < 0.001$; n = 56)	
Host-encoded miRNAs		
hsa-miR-10a-5p	hsa-miR-10b-5p ($\varrho = 0.68$, $p < 0.001$; n = 71)	
	hsa-miR-22-5p ($\varrho = 0.62$, $p < 0.001$; n = 71)	
	hsa-miR-26b-5p ($\varrho = 0.58$, $p < 0.001$; n = 71)	
	hsa-miR-181d-5p ($\varrho = 0.37$, $p = 0.001$; n = 71)	
	hsa-miR-192-5p ($\varrho = 0.68$, $p < 0.001$; n = 71)	
	hsa-miR-532-5p ($\varrho = 0.69$, $p < 0.001$; n = 71)	
	hsa-let-7i-5p ($\varrho = 0.68$, $p < 0.001$; n = 71)	
hsa-miR-26b-5p	hsa-miR-10b-5p ($\varrho = 0.75$, $p < 0.001$; n = 71)	
	hsa-miR-22-5p ($\varrho = 0.65$, $p < 0.001$; n = 71)	
	hsa-miR-181d-5p ($\varrho = 0.42$, $p < 0.001$; n = 71)	
	hsa-miR-192-5p ($\varrho = 0.77$, $p < 0.001$; n = 71)	
	hsa-miR-200b-5p ($\varrho = 0.26$, $p = 0.028$; n = 71)	
	hsa-miR-532-5p ($\varrho = 0.84$, $p < 0.001$; n = 71)	
	hsa-let-7i-5p ($\varrho = 0.84$, $p < 0.001$; n = 71)	
hsa-miR-181d-5p	hsa-miR-10b-5p ($\varrho = 0.38$, $p = 0.001$; n = 71)	
	hsa-miR-22-5p ($\varrho = 0.42$, $p < 0.001$; n = 71)	
	hsa-miR-192-5p ($\varrho = 0.37$, $p = 0.002$; n = 71)	
	hsa-miR-499a-5p ($\varrho = 0.28$, $p = 0.019$; n = 71)	
	hsa-miR-532-5p ($\varrho = 0.48$, $p < 0.001$; n = 71)	
	hsa-let-7i-5p ($\varrho = 0.49$, $p < 0.001$; n = 71)	
hsa-let-7i	hsa-miR-10b-5p ($\varrho = 0.77$, $p < 0.001$; n = 71)	
	hsa-miR-22-5p ($\varrho = 0.80$, $p < 0.001$; n = 71)	
	hsa-miR-26b-5p ($\varrho = 0.84$, $p < 0.001$; n = 71)	
	hsa-miR-181d-5p ($\varrho = 0.49$, $p < 0.001$; n = 71)	
	hsa-miR-192-5p ($\varrho = 0.83$, $p < 0.001$; n = 71)	
	hsa-miR-200b-5p ($\varrho = 0.26$, $p = 0.026$; n = 71)	
	hsa-miR-532-5p ($\varrho = 0.91$, $p < 0.001$; n = 71)	
EBV-encoded miRNAs		
ebv-miR-BART1-5p	hsa-miR-4435 ($\varrho = 0.42$, $p = 0.017$; n = 32)	ebv-miR-BART20-5p ($\varrho = -0.53$, $p = 0.014$; n = 21)
ebv-miR-BART2-5p	ebv-miR-BART20-5p ($\varrho = 0.55$, $p = 0.007$; n = 22)	hsa-miR-200b-5p ($\varrho = -0.32$, $p = 0.048$; n = 39)
	ebv-miR-BHRF1-3 ($\varrho = 0.70$, $p = 0.005$; n = 15)	
ebv-miR-BART20-5p		hsa-miR-26b-5p ($\varrho = -0.48$, $p = 0.002$; n = 42)
		hsa-let-7i-5p ($\varrho = -0.32$, $p = 0.039$; n = 42)

2.4. Impact of B-Cell Depletion Therapies

To determine whether BCDTs affected the expression of host-encoded miRNAs in sera from PwMS, miRNA sequencing profiles from the DC were analyzed by machine-learning models. These analyses were compared between three subgroups, including BCDT-treated PwMS, non-BCDT-treated PwMS, and PwoMS. Machine learning identified the top 12 differentially expressed host-encoded miRNAs across the groups (Figure 4A). Among these 12 miRNAs, hsa-miR-10b-5p, hsa-miR-26b-5p, hsa-miR-192-5p, hsa-miR-532-5p, and hsa-let-7i-

5p were significantly differentially expressed between BCDT- and non-BCDT-treated PwMS and PwoMS in the DC (Figures 4B and S3A–D). However, only mean hsa-miR-26b-5p showed suppressed levels in the non-BCDT-treated PwMS group in both the DC (Figure 4B; read difference = 778.9; 95%CI = 162.8–1395; $p < 0.05$, $q < 0.01$) and VC (Figure 4C; copy difference = 727; 95%CI = 560.1–6895; $p < 0.05$, $q < 0.01$) compared to PwoMS. In ROC analysis comparing non-BCDT-treated PwMS with PwoMS, hsa-miR-26b-5p exhibited a significant discriminatory ability (AUROC = 0.78 in DC and 0.70 in VC, $p < 0.05$; Supplementary Figure S3E).

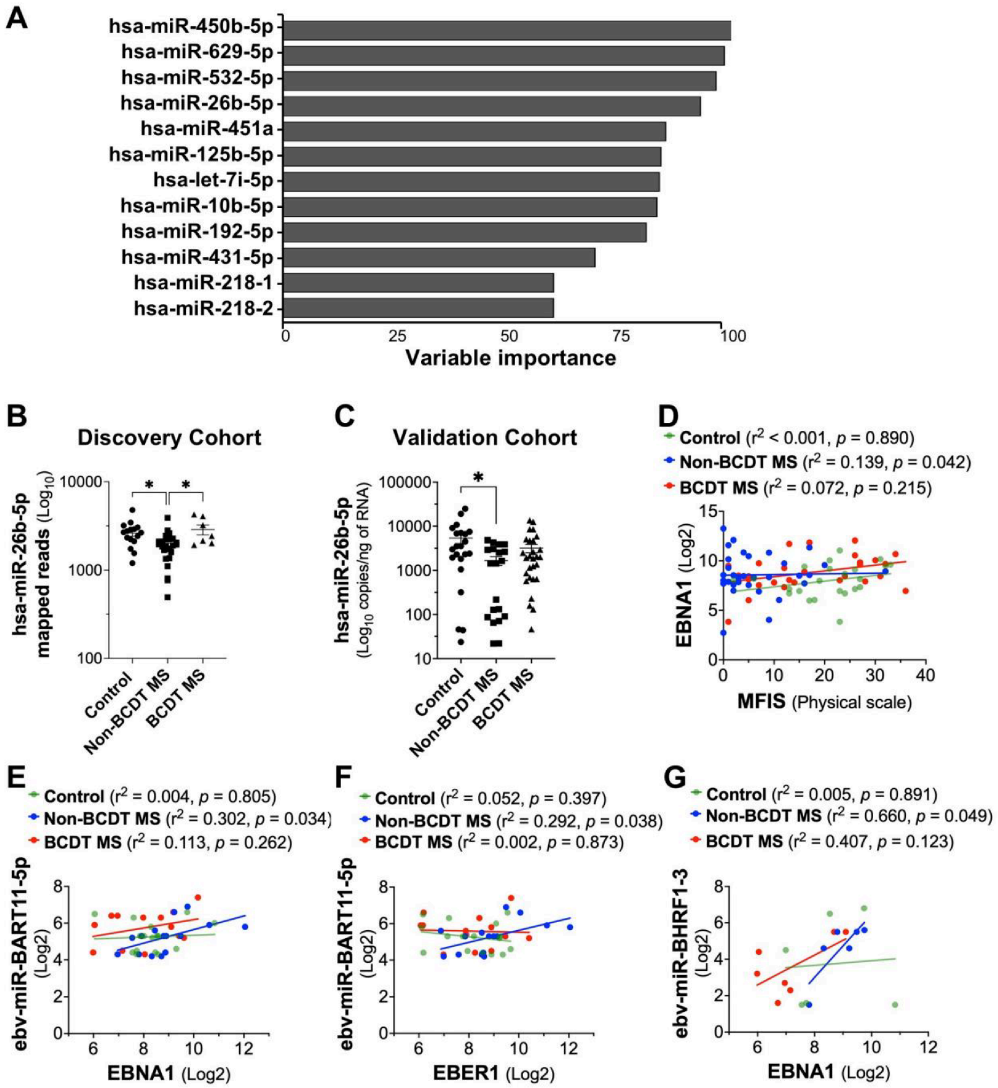

Figure 4. Impact of B-cell depletion therapies (BCDTs) on serum viral- and host-encoded miRNAs. (**A**) Identification of BCDT-associated host-encoded miRNAs used variable importance scores from a multivariate machine-learning model to identify the top 12 host-encoded miRNAs that differentiate PwMS receiving BCDT from those not receiving BCDT (non-BCDT) and from PwoMS in the Discovery Cohort. (**B**,**C**) Host-encoded miRNA expression, showing differential expression of the identified host-encoded miRNAs (**B**) was profiled by sequencing in the Discovery Cohort; one-way ANOVA with Tukey's post hoc test ($F(2,45) = 7.2$, $p = 0.002$) and (**C**) verified by ddPCR in the Validation Cohort; one-way ANOVA with Tukey's post hoc test ($F(2,67) = 4.1$, $p = 0.02$. Data are presented as mean ± SEM; * $p < 0.05$ for comparison between control and non-BCDT-treated PwMS. (**D**–**G**) Linear regression (r^2) analysis in the Validation Cohort displayed association(s) between (**D**) *EBNA1* copy number and MFIS (physical scale), (**E**,**F**) levels of ebv-miR-BART11-5p and (**E**) *EBNA1* copy number, and (**F**) *EBER1* copy number, (**G**) levels of ebv-miR-BHRF1-3 and *EBNA1* copy number in non-BCDT-treated PwMS compared to PwoMS ($p < 0.05$).

As B cells are the primary reservoir for EBV [4], the effects of BCDT status on EBV viremia and miRNA levels were investigated in combined cohorts, disclosing that the *EBNA1*-encoded DNA copy number was correlated with MFIS in the non-BCDT-treated PwMS group (Figure 4D; $r^2 = 0.14$; 95%CI = 0.002–0.1; $p < 0.05$, $q < 0.05$; n = 31). In the VC, linear regressions indicated that increased levels of ebv-miR-BART11-5p correlated with *EBNA1* copy number (Figure 4E; $r^2 = 0.3$; 95%CI = 0.03–0.7; $p < 0.05$, $q < 0.05$; n = 15) and *EBER1* copy number (Figure 4F; $r^2 = 0.3$; 95%CI: 0.02–0.63; $p < 0.05$, $q < 0.05$; n = 15) while ebv-BHRF1-3 levels were associated with *EBNA1* levels (Figure 4G; $r^2 = 0.7$; 95%CI = 0.01–3.5; $p < 0.05$, $q < 0.05$; n = 6) in the non-BCDT-treated PwMS group. In the BCDT-treated PwMS group, age was correlated with *EBNA1* levels (combined cohorts: $r^2 = 0.2$; 95%CI = 0.01–0.2; $p < 0.05$, $q < 0.05$; n = 25) and ebv-miR-BART2-5p levels (VC: $r^2 = 0.3$; 95%CI = 0.02–0.2; $p < 0.05$, $q < 0.05$; n = 17) (Supplementary Figure S4). These data suggested an association between BCDT treatment and both EBV viremia and viral miRNA levels; however, whether BCDTs directly influence EBV viremia or miRNA levels could not be determined from our data.

3. Discussion

This study is the first report of serum viral and host miRNA profiling with concurrent EBV DNA levels in PwMS versus PwoMS as controls that has identified specific viral and host miRNAs associated with EBV viremia, disease severity, and BCDT-treated status. Our findings reveal that a previously unrecognized miRNA, hsa-miR-181d-5p, was suppressed in sera from PwMS in both the DC and VC. Consistent with the previous association of hsa-miR-26b-5p with PwMS, the present study further revealed that treatment status (BCDT) was associated with serum miRNA expression [19]. Indeed, both host miRNAs targeted multiple genes that implicate metabolic and NOD-like receptor signaling pathways, e.g., MAT2A, NAMPT, and NEK7, which were induced in the cerebral white matter of PwMS. Similar relationships between miRNAs and their targets have been reported in human brain tissues [20,21]. Dysregulated EBV- and host-encoded miRNAs were associated with PwMS EDSS score, as well as EBV viremia, fatigue, and responses to therapy. However, it is important to note that the detection of circulating EBV DNA reflects viral shedding and does not necessarily indicate active viral replication or lytic infection.

In the present study, ebv-miR-BART11-5p levels were elevated in PwMS with low disability compared to high disability. This finding might indicate a dynamic change in viral miRNA expression over the disease course. Specifically, ebv-miR-BART11-5p, which is involved in regulating B-cell differentiation [22] or evading immune surveillance [23], showed higher expression in earlier (and less severe) stages of disease. Viral miRNAs, including ebv-miR-BART1-5p, ebv-miR-BART2-5p, ebv-miR-BART20-5p, and ebv-miR-BHRF1-3, were detectable in the serum of both PwMS and PwoMS participants, suggesting that their mere detection is not a specific biomarker for MS. However, their expression and associations with clinical variables, such as age, disease duration, and fatigue, within the PwMS group implied disease-specific dysregulation. The current results were consistent with a previous study that reported the detection of these viral miRNAs in plasma exosomes and whole blood from MS patients [15].

The reduction of hsa-miR-26b-5p levels in PwMS with high EDSS is consistent with previous studies, which reported dysregulation of hsa-miR-26b-5p in PBMCs from PwMS [19]. Notably, hsa-miR-181d-5p, which was also found to be suppressed in the DC and VC, has also been implicated in chronic autoimmune diseases such as Sjögren's syndrome patients [24]. These common findings strengthen the evidence for the involvement of these host miRNAs in MS pathogenesis. Although these miRNAs showed discriminatory ability in specific subgroup analyses, the overall out-of-sample performance was modest. They

therefore represent candidate biomarkers rather than clinically validated diagnostic tools, and validation in larger, prospective cohorts will be required.

BCDTs, including anti-CD20 antibodies such as ocrelizumab, rituximab, ublituximab, and ofatumumab, deplete circulating B cells [25]. This depletion could modulate EBV viremia, given that B cells are a major reservoir of EBV, as well as the profiles of both viral and host miRNAs in serum. Nonetheless, the present study showed no differences in EBV viremia between PwMS, receiving or not receiving BCDTs, despite stratification by disease severity. Since B cells are a primary reservoir for EBV [5], this finding suggests that the quantity of circulating cell-free EBV DNA might not be a distinguishing feature in these cohorts but rather should be considered merely a marker for viral infection or perhaps reactivation [26]. A longitudinal study recently reported EBNA1 antibody titers in MS, MOGAD, and NMOSD, suggesting that high levels of EBNA-1 peptide antibody titers might discriminate MS from other neuroinflammatory diseases [27]. In PwMS not receiving BCDTs, ebv-miR-BART11-5p and ebv-miR-BHRF1-3 showed a positive association with EBV viremia. This exploratory correlation suggests that in the absence of BCDTs, these viral miRNAs might be associated with viral production. This is consistent with the known function of ebv-miR-BHRF1-3, which targets BZLF1, a key viral gene driving lytic replication [14], while ebv-miR-BART11-5p regulates B-cell differentiation and could modulate the host environment during infection [22]. Additionally, age-related increases in both EBV DNA loads and ebv-miR-BART2-5p levels were consistent with immune senescence and the age-related reactivation of latent viruses [28]. Notably, ebv-miR-BART2-5p targets the viral DNA polymerase BALF5, suggesting its increased expression might be related to viral reactivation in an aging immune system [12].

Given that fatigue is a common symptom in both EBV infection and MS [16–18], this study demonstrates that fatigue was elevated in PwMS, especially among those with high EDSS scores. This finding was aligned with correlations between fatigue and both EDSS and disease duration. The associations between viral and host factors with fatigue varied by EDSS and BCDT treatment status, suggesting that fatigue in MS may be driven by multiple biological mechanisms. The association between EBV-encoded *EBNA1* DNA levels and psychosocial fatigue in the Low-EDSS PwMS, and with physical fatigue in non-BCDT-treated PwMS, provides further evidence for a potential role of EBV in MS-related fatigue. This finding is also aligned with a previous report of increased IgG reactivity against EBNA1 in patients with chronic fatigue syndrome in PBMCs and plasma [18]. Further supporting a role of EBV, this study showed that ebv-miR-BART1-5p correlated with physical fatigue, while ebv-miR-BART20-5p correlated with psychosocial fatigue, specifically in low-disability PwMS.

This study has several limitations. In some analyses, miRNAs were not detectable, presumably because they were below the sensitivity levels for the miRNA sequencing or ddPCR assays; nonetheless, an undetectable result does not indicate that the miRNAs were absent, but could reflect technical constraints due to low-input transcriptomics (e.g., RNA yield, reverse transcription efficiency, or ddPCR amplification thresholds). Assigning an arbitrary value of zero or applying categorical tests (e.g., chi-squared) would treat an unknown concentration as an exact measurement, introducing artificial variance and bias into the analysis and potentially distorting the distribution and quantitative comparisons. For this reason, and to maintain analytical rigor, only detectable samples were included in the continuous quantitative models. Second, the sample size was relatively small, particularly for exploratory correlation analyses, which limits statistical power and the reliability of weak correlations. Third, treatment status was unevenly distributed across disability groups and differed between cohorts. A single High-EDSS PwMS in the Discovery Cohort was BCDT-treated and thus, adjustment for treatment was not feasible in that cohort; although

treatment status was adjusted for in the Validation Cohort, residual confounding cannot be excluded, and some EDSS-related associations in the Discovery Cohort may partly reflect differences in BCDT status rather than disability itself. Fourth, our findings were exploratory and associative without performing functional experiments to validate the mechanistic relationships proposed herein, because this was not purpose of the study. However, the target proteins were identified using the TarBase v9.0 database and their functions annotated from previous our study [11] merit further analyses. Fifth, technical replicates were not performed for the ddPCR analyses; although ddPCR provides high sensitivity, the lack of replicates might limit the precision of quantification for low-abundance EBV miRNAs. Finally, RNA quality control, including hemolysis and exogenous spike-in controls, was not directly assessed; thus, low-level hemolysis and variations in RNA extraction efficiency cannot be excluded. Total RNA was quantified by NanoDrop prior to cDNA synthesis, which could overestimate RNA concentration in serum samples. These limitations should be considered when interpreting the results and validation in larger cohorts with improved detection sensitivity is warranted in the future.

In conclusion, this study profiled serum viral and host miRNAs in matched PwMS and PwoMS that were associated with EBV viremia, treatment regimens, and disease severity. These analyses revealed associations between viral and host miRNA expression, including correlates with BCDT, targeted brain proteins, and other clinical parameters. Additionally, hsa-miR-26b-5p and hsa-miR-181d-5p were promising candidate biomarkers for MS because they showed consistent differential expression across both the Discovery and Validation Cohorts. Moreover, the present discoveries regarding the viral miRNAs detected in serum offer new avenues for understanding host–viral interactions, disease onset and progression, as well as responses to therapy in PwMS.

4. Materials and Methods

4.1. Ethics

Participants were enrolled at the Universities of Alberta and Calgary from July 2021 to July 2023. The study protocol was approved by the University of Alberta (Protocol No. pSITE00000007) and the University of Calgary Health Research Ethics Board (Protocol No. REB20-1034), date of approval 11 March 2021. All participants provided written informed consent.

4.2. Clinical Cohorts and Study Design

Serum samples were collected as part of the Alberta's Tomorrow MS Project from PwMS and PwoMS (healthy controls without neurological or autoimmune diseases); participants who were matched by sex, age, and from the same geographically-based population (Table 1). The diagnosis of MS was predicated on the MacDonald 2017 criteria [29]. Fatigue was assessed using the Modified Fatigue Impact Scale (MFIS), which evaluated the impact of fatigue in the past 4 weeks [30]. The study was designed as a Discovery Cohort (DC; n = 48) and a Validation Cohort (VC; n = 71) (Figure 1). PwMS were categorized by two independent grouping variables: disability levels (using the Expanded Disability Status Scale (EDSS) with a cutoff score of less than 3.0 to define low versus high disability; Table 1), and treatment status (BCDT- vs. non-BCDT-treated; Supplementary File S1). These variables were analyzed separately. Because treatment status was unevenly distributed across disability groups and cohorts, the potential for confounding by treatment exposure is acknowledged as a limitation. Serum samples were isolated by centrifugation at the Alberta's Tomorrow MS Project biobank and stored at −80 °C before being shipped to the University of Alberta. Samples were not subjected to repeated freeze–thaw cycles prior analysis.

4.3. Nucleic Acid Isolation and cDNA Synthesis

DNA was extracted from serum using a modification of the DNeasy Blood & Tissue Kit (Qiagen, Cat no. 69504) protocol for non-nucleated blood. In brief, 200 µL of serum was incubated with 20 µL of proteinase K solution and 200 µL of buffer AL for 2 h at 56 °C, followed by the manufacturer's protocol for binding and washing. Elution was performed with 14 µL of elution buffer and the membrane for 10 min. This elution was performed twice per sample to maximize DNA recovery. Total RNA, including miRNAs, was extracted with the miRNeasy Serum/Plasma Advanced Kit (Qiagen, Cat no. 217204) following the manufacturer's protocol. The concentration of total RNA was measured using a NanoDrop spectrophotometer (ND-1000, NanoDrop Technologies). For cDNA synthesis, 10 ng of total RNA was reverse transcribed using miRCURY LNA RT Kit (Qiagen, Cat no. 339340), according to the manufacturer's instructions. cDNA was diluted 1:60 (v/v) with nuclease-free water before analysis [31].

4.4. Small RNA Sequencing

Small RNA sequencing libraries were constructed from RNA isolated from 48 samples in the DC to profile miRNA expression. All library preparation and sequencing were performed by the molecular biology and functional genomics platform at the Institut de Recherches Cliniques de Montréal (IRCM; QC, Canada). Sequencing was conducted on an Illumina NextSeq 2000, generating 100-base single reads (Illumina, San Diego, CA, USA). Raw sequencing reads were processed using miRDeep2 to quantify miRNA abundances. The data were expressed as read counts normalized to the total library size for each sample [31]. The sequencing datasets generated and analyzed during the current study have been deposited in the Gene Expression Omnibus (GEO) database under accession number GSE347948.

4.5. Machine Learning

To identify virus–host interactions in PwMS, machine learning was applied to the DC. The analysis included clinical variables (Table 1), EBV *EBNA1* and *EBER1* copies/mL, and miRNA sequencing data. First, following false discovery rate-corrected univariate tests to identify the serum collection site as a confounder, miRNAs with sparse expression were excluded by retaining only those detected in at least 10 samples per group. Next, differential expression analysis accounting for the collection site effect was performed across the cohort, and the collection-site-adjusted significant miRNAs were carried forward for modeling. Principal component analysis was used for dimensionality, and the first 20 components (>85% of the total variance) were used to prioritize 30 miRNAs for classification modeling. Five models, including least absolute shrinkage and selection operator (LASSO), random forest (RF), support vector machine (SVM), linear discriminant analysis (LDA), and neural discriminant analysis (NDA), were trained. Important miRNAs identified by each model were compared across models, and overlapping features were prioritized. The variable importance of selected miRNAs was subsequently assessed using linear and nonlinear models.

To assess out-of-sample classification performance while limiting information leakage, we performed repeated nested cross-validation. In the repeated nested cross-validation analysis, mean balanced accuracy across classifiers ranged from 0.40 to 0.43, macro-F1 from 0.39 to 0.41, and multiclass AUROC from 0.59 to 0.60 with training-set-based site adjustment. Without post-selection site adjustment, balanced accuracy ranged from 0.31 to 0.34 and multiclass AUROC from 0.48 to 0.52. These findings indicate modest classification performance that was sensitive to site handling. The outer assessment used stratified 4-fold cross-validation repeated 20 times. Within each outer training set, miRNA filtering and

feature ranking were repeated using the training data only, and the top candidate features were selected before model fitting. Model-specific hyperparameters were subsequently tuned using 3-fold inner cross-validation. The held-out outer test samples were not used for either feature selection or hyperparameter tuning. Performance was summarized using balanced accuracy, macro-F1, and multiclass AUROC. Because collection sites were strongly imbalanced across clinical groups, performance was evaluated both with training-set-based site adjustment and in a sensitivity analysis without post-selection site adjustment. The cross-validation procedure, performance metrics, and analysis code are shown in Supplementary File S3.

4.6. Droplet Digital PCR Analysis

EBV DNA encoding *EBNA1* and *EBER1*, and miRNA levels were quantified using droplet digital PCR (ddPCR). Viral DNA levels were measured in sera from both the Discovery and Validation Cohorts. EBV- and host-encoded miRNA levels were quantified in the Validation Cohort. Five µL of DNA or diluted cDNA was used as a template along with target-specific primers (Supplementary File S2) and QX200 ddPCR EvaGreen Supermix (Bio-Rad, Mississauga, ON L5T 1C9, Canada). Droplets were generated using a QX200 Droplet Generator (Bio-Rad). PCR amplification was performed using the following program: an initial activation at 95 °C for 10 min, denaturation at 94 °C for 30 s, and annealing at 58 °C for 1 min (40 cycles). Droplets were read on a QX200 Droplet Reader (Bio-Rad). Data were analyzed with QuantaSoft Analysis Pro 1.0.596 software (Bio-Rad). The fluorescence threshold was set manually based on the negative droplet population from a no-template control. EBV DNA loads were expressed as absolute copies per milliliter of serum. MicroRNA expression levels were presented as absolute copies per nanogram of RNA. A no-template control was included to establish the fluorescence threshold [32]. Values below the established fluorescence threshold were defined as zero for viral DNA and as undetectable for miRNA levels: samples with fewer than three positive droplets were considered below the limit of detection and defined as undetectable.

Technical replicates were not performed for the ddPCR analyses. Given the limitation of low-input clinical samples and limited RNA yield, this study prioritized biological replicates over technical replicates to preserve statistical power at the group level. Undetectable miRNA results cannot be conflated with a true target value of zero; an undetectable result may reflect technical variables inherent to low-input transcriptomics, e.g., RNA extraction yield, reverse transcription efficiency, or ddPCR amplification thresholds, rather than a complete absence of expression. Assigning an arbitrary value of zero would treat an unknown concentration as an exact measurement and introduce artificial variance and bias into quantitative analyses. Therefore, detectable miRNA targets were included in the continuous quantitative model rather using assigned arbitrary values. The number and percentage of detectable results for each miRNA and study group are reported in Supplementary File S4. Detectable miRNA targets were included in the analyses, as described in the Section 4.8.

4.7. Identification of Host Genes in the Brain Targeted by miRNAs

Putative target genes of EBV- and host-encoded miRNAs were predicted using TarBase v9.0 [33]. A microT score threshold of ≥0.9 was used for host-encoded miRNAs, and targets meeting this criterion were retained. Host genes targeted by identified miRNAs were analyzed in a publicly available dataset from our group that encoded proteins showing significant upregulation in cerebral white matter from PwMS (n = 8) compared to PwoMS (n = 8) (MassIVE: MSV000096790) [11].

4.8. Statistical Analysis

Statistical and machine-learning analyses were performed using R (version 4.5.0) and GraphPad Prism (version 10). Statistical significance was defined as * $p < 0.05$ and ** $p < 0.01$ (two-tailed test). To account for multiple comparisons, the FDR correction was applied using the Benjamini–Hochberg test. The FDR-adjusted q-value of <0.05 was considered statistically significant, in addition to p-value. Categorical variables, including collection site and sex, were compared between groups using the chi-squared test. Continuous variables, including age, EDSS, disease duration, viral load, MFIS, and miRNA expression, were analyzed using the Kruskal–Wallis test with false discovery rate (FDR) correction, the Mann–Whitney U test, or one-way ANOVA followed by Tukey's post hoc test. The association between miRNAs, EBV DNA load, and clinical variables was assessed using linear regression (r^2) and Spearman's correlation coefficient (ϱ), with 95% confidence intervals (CIs). For miRNA measurement, undetectable values (zero count in sequencing data and below the established threshold in ddPCR) were excluded from analyses. For group comparisons, exclusion was applied per target. For correlation and linear regression, pairwise deletion was used: each analysis included only samples with detectable values for all variables in that model. The diagnostic performance of miRNAs for discriminating between groups was assessed using a receiver operating characteristic (ROC) curve. The area under the receiver operating characteristic curve (AUROC), sensitivity, specificity, and 95% CIs were calculated.

Supplementary Materials: The following supporting information can be downloaded at: https://www.mdpi.com/article/10.3390/ijms272310602/s1.

Author Contributions: D.O. drafted and revised the manuscript, analyzed and interpreted data, and designed the study. N.Z. and U.Z.S. analyzed and interpreted data. W.G.B. and E.A.C. processed, analyzed and interpreted data. H.M.M., N.N., P.D., J.P., P.S. and L.K. interpreted data. C.C.-L. conceived the study and interpreted data. C.P. supervised the overall study, conceived the study, drafted and revised the manuscript. All authors have read and agreed to the published version of the manuscript.

Funding: These studies were supported by funds to the Alberta Multiple Sclerosis Collaboration from the Alberta Jobs, Economy and Innovation Economic Policy and Strategy Division, and the University Hospital Foundation MS Team Grant (RES0050293). CP is supported by the Henri M. Toupin Chair in Neurocognitive Disorders (CP) (RES0065116). DO is supported by a Mathematics of Information Technology and Complex Systems Fellowship (MI MA IT45634).

Institutional Review Board Statement: The study protocols were approved by the University of Alberta (Protocol No. pSITE00000007) and the University of Calgary Health Research Ethics Board (Protocol No. REB20-1034), date of approval 11 March 2021. All procedures were conducted in accordance with the TCPS 2 (2022) Tri-Council Policy Statement (aligned with the core ethical values of the Declaration of Helsinki), ICH E6 Good Clinical Practice (GCP), and Part C, Division 5 of the Canadian Food and Drug Regulations. Questionnaires and clinical data were collected after obtaining voluntary informed consent from all participants.

Informed Consent Statement: All participants provided written informed consent.

Data Availability Statement: The data presented in this study are available on request from the corresponding author due to individual participant data will not be shared publicly because informed consent and ethical approval did not cover public data sharing. The sequencing datasets generated and analyzed during the current study have been deposited in the Gene Expression Omnibus (GEO) database under accession number GSE347948.

Acknowledgments: The authors thank the members of the Brain Power lab at the University of Alberta, as well as the IRCM molecular and functional genomics platform, for their assistance.

Conflicts of Interest: The authors declare no conflict of interest.

Abbreviations

BCDT: B-cell depletion therapy; DC: Discovery Cohort; ddPCR: Droplet digital PCR; EBV: Epstein–Barr virus; EDSS: Expanded Disability Status Scale; miR: MicroRNA; MFIS: Modified Fatigue Impact Scale; MS: Multiple sclerosis; PwMS: Persons with multiple sclerosis; PwoMS: Persons without multiple sclerosis; VC: Validation Cohort.

References

1. Hauser, S.L. Advances in Multiple Sclerosis. *N. Engl. J. Med.* **2026**, *395*, 54–68. [CrossRef] [PubMed]
2. Waubant, E.; Lucas, R.; Mowry, E.; Graves, J.; Olsson, T.; Alfredsson, L.; Langer-Gould, A. Environmental and genetic risk factors for MS: An integrated review. *Ann. Clin. Transl. Neurol.* **2019**, *6*, 1905–1922. [CrossRef] [PubMed]
3. Bjornevik, K.; Cortese, M.; Healy, B.C.; Kuhle, J.; Mina, M.J.; Leng, Y.; Elledge, S.J.; Niebuhr, D.W.; Scher, A.I.; Munger, K.L.; et al. Longitudinal analysis reveals high prevalence of Epstein-Barr virus associated with multiple sclerosis. *Science* **2022**, *375*, 296–301. [CrossRef] [PubMed]
4. Serafini, B.; Rosicarelli, B.; Franciotta, D.; Magliozzi, R.; Reynolds, R.; Cinque, P.; Andreoni, L.; Trivedi, P.; Salvetti, M.; Faggioni, A.; et al. Dysregulated Epstein-Barr virus infection in the multiple sclerosis brain. *J. Exp. Med.* **2007**, *204*, 2899–2912. [CrossRef] [PubMed]
5. Babcock, G.J.; Decker, L.L.; Freeman, R.B.; Thorley-Lawson, D.A. Epstein-Barr virus-infected resting memory B cells, not proliferating lymphoblasts, accumulate in the peripheral blood of immunosuppressed patients. *J. Exp. Med.* **1999**, *190*, 567–576. [CrossRef] [PubMed]
6. Lee, D.S.W.; Rojas, O.L.; Gommerman, J.L. B cell depletion therapies in autoimmune disease: Advances and mechanistic insights. *Nat. Rev. Drug Discov.* **2021**, *20*, 179–199. Correction in *Nat. Rev. Drug Discov.* **2025**, *24*, 72. [CrossRef] [PubMed]
7. Portaccio, E.; Magyari, M.; Havrdova, E.K.; Ruet, A.; Brochet, B.; Scalfari, A.; Di Filippo, M.; Tur, C.; Montalban, X.; Amato, M.P. Multiple sclerosis: Emerging epidemiological trends and redefining the clinical course. *Lancet Reg. Health Eur.* **2024**, *44*, 100977. [CrossRef] [PubMed]
8. Montalban, X.; Lebrun-Frénay, C.; Oh, J.; Arrambide, G.; Moccia, M.; Amato, M.P.; Amezcua, L.; Banwell, B.; Bar-Or, A.; Barkhof, F.; et al. Diagnosis of multiple sclerosis: 2024 revisions of the McDonald criteria. *Lancet Neurol.* **2025**, *24*, 850–865. [CrossRef] [PubMed]
9. O'Brien, J.; Hayder, H.; Zayed, Y.; Peng, C. Overview of microRNA biogenesis, mechanisms of actions, and circulation. *Front. Endocrinol.* **2018**, *9*, 402. [CrossRef] [PubMed]
10. Condrat, C.E.; Thompson, D.C.; Barbu, M.G.; Bugnar, O.L.; Boboc, A.; Cretoiu, D.; Suciu, N.; Cretoiu, S.M.; Voinea, S.C. MiRNAs as biomarkers in disease: Latest findings regarding their role in diagnosis and prognosis. *Cells* **2020**, *9*, 276. [CrossRef] [PubMed]
11. Wang, H.; Pollock, N.M.; Miranzadeh Mahabadi, H.; Patel, J.; Moussa, E.W.; Fernandes, J.P.; Branton, W.G.; Zhang, N.; Elliott, C.; Schmitt, L.; et al. Brain and neural cell type proteomics reveal extracellular matrix proteins enriched in progressive multiple sclerosis. *Nat. Commun.* **2026**, *17*, 1368. [CrossRef] [PubMed]
12. Barth, S.; Pfuhl, T.; Mamiani, A.; Ehses, C.; Roemer, K.; Kremmer, E.; Jäker, C.; Höck, J.; Meister, G.; Grässer, F.A. Epstein-Barr virus-encoded microRNA miR-BART2 down-regulates the viral DNA polymerase BALF5. *Nucleic Acids Res.* **2008**, *36*, 666–675. [CrossRef] [PubMed]
13. Jung, Y.J.; Choi, H.; Kim, H.; Lee, S.K. MicroRNA miR-BART20-5p stabilizes Epstein-Barr virus latency by directly targeting BZLF1 and BRLF1. *J. Virol.* **2014**, *88*, 9027–9037. [CrossRef] [PubMed]
14. Fachko, D.N.; Chen, Y.; Skalsky, R.L. Epstein-Barr virus miR-BHRF1-3 targets the BZLF1 3'UTR and regulates the lytic cycle. *J. Virol.* **2022**, *96*, e0149521. [CrossRef] [PubMed]
15. Hvalkof, V.H.; Olsson, A.G.S.; Gustavsen, S.; Langkilde, A.R.; Hansen, M.B.; Sellebjerg, F.; Søndergaard, H.B. Profiling of Epstein-Barr virus microRNAs in whole blood and exosomes in multiple sclerosis. *Immunol. Investig.* **2025**, *54*, 1524–1541. [CrossRef] [PubMed]
16. Braley, T.J.; Chervin, R.D. Fatigue in multiple sclerosis: Mechanisms, evaluation, and treatment. *Sleep* **2010**, *33*, 1061–1067. [CrossRef] [PubMed]
17. White, P.D.; Thomas, J.M.; Amess, J.; Crawford, D.H.; Grover, S.A.; Kangro, H.O.; Clare, A.W. Incidence, risk and prognosis of acute and chronic fatigue syndromes and psychiatric disorders after glandular fever. *Br. J. Psychiatry* **1998**, *173*, 475–481. [CrossRef] [PubMed]
18. Shikova, E.; Reshkova, V.; Kumanova, A.; Raleva, S.; Alexandrova, D.; Capo, N.; Murovska, M. Cytomegalovirus, Epstein-Barr virus, and human herpesvirus-6 infections in patients with myalgic encephalomyelitis/chronic fatigue syndrome. *J. Med. Virol.* **2020**, *92*, 3682–3688. [CrossRef] [PubMed]

19. Sanders, K.A.; Benton, M.C.; Lea, R.A.; Maltby, V.E.; Agland, S.; Griffin, N.; Scott, R.J.; Tajouri, L.; Lechner-Scott, J. Next-generation sequencing reveals broad down-regulation of microRNAs in secondary progressive multiple sclerosis CD4$^+$ T cells. *Clin. Epigenet.* **2016**, *8*, 87. [CrossRef] [PubMed]
20. Boudreau, R.L.; Jiang, P.; Gilmore, B.L.; Spengler, R.M.; Tirabassi, R.; Nelson, J.A.; Ross, C.A.; Xing, Y.; Davidson, B.L. Transcriptome-wide discovery of microRNA binding sites in human brain. *Neuron* **2014**, *81*, 294–305. [CrossRef] [PubMed]
21. Nowakowski, T.J.; Rani, N.; Golkaram, M.; Zhou, H.R.; Alvarado, B.; Huch, K.; West, J.A.; Leyrat, A.; Pollen, A.A.; Kriegstein, A.R.; et al. Regulation of cell-type-specific transcriptomes by microRNA networks during human brain development. *Nat. Neurosci.* **2018**, *21*, 1784–1792. [CrossRef] [PubMed]
22. Ross, N.; Gandhi, M.K.; Nourse, J.P. The Epstein-Barr virus microRNA BART11-5p targets the early B-cell transcription factor EBF1. *Am. J. Blood Res.* **2013**, *3*, 210–224. [PubMed]
23. Wang, J.; Ge, J.; Wang, Y.; Xiong, F.; Guo, J.; Jiang, X.; Zhang, L.; Deng, X.; Gong, Z.; Zhang, S.; et al. EBV miRNAs BART11 and BART17-3p promote immune escape through the enhancer-mediated transcription of PD-L1. *Nat. Commun.* **2022**, *13*, 866. [CrossRef] [PubMed]
24. Castro, I.; Carvajal, P.; Jara, D.; Aguilera, S.; Heathcote, B.; Barrera, M.-J.; Aliaga-Tobar, V.; Maracaja-Coutinho, V.; Urzúa, U.; Quest, A.F.G.; et al. Small RNA expression profiling reveals hsa-miR-181d-5p downregulation associated with TNF-α overexpression in Sjögren's syndrome patients. *Front. Immunol.* **2022**, *13*, 870094. [CrossRef] [PubMed]
25. Montalvao, F.; Garcia, Z.; Celli, S.; Breart, B.; Deguine, J.; Van Rooijen, N.; Bousso, P. The mechanism of anti-CD20-mediated B cell depletion revealed by intravital imaging. *J. Clin. Investig.* **2013**, *123*, 5098–5103. [CrossRef] [PubMed]
26. Cocuzza, C.E.; Piazza, F.; Musumeci, R.; Oggioni, D.; Andreoni, S.; Gardinetti, M.; Fusco, L.; Frigo, M.; Banfi, P.; Rottoli, M.R.; et al. Quantitative detection of Epstein-Barr virus DNA in cerebrospinal fluid and blood samples of patients with relapsing-remitting multiple sclerosis. *PLoS ONE* **2014**, *9*, e94497. Correction in *PLoS ONE* **2014**, *9*, e103890. [CrossRef] [PubMed]
27. Vietzen, H.; Kühner, L.M.; Berger, S.M.; Reinecke, R.; Rostásy, K.; Saucke, H.; Kauth, F.; Koukou, G.; Sommer, S.; Wendel, E.-M.; et al. Epstein-Barr Virus antibodies to differentiate Multiple Sclerosis from other neuroinflammatory diseases. *JAMA Neurol.* **2026**, *83*, 461–470. [CrossRef] [PubMed]
28. Stowe, R.P.; Kozlova, E.V.; Yetman, D.L.; Walling, D.M.; Goodwin, J.S.; Glaser, R. Chronic herpesvirus reactivation occurs in aging. *Exp. Gerontol.* **2007**, *42*, 563–570. [CrossRef] [PubMed]
29. Thompson, A.J.; Banwell, B.L.; Barkhof, F.; Carroll, W.M.; Coetzee, T.; Comi, G.; Correale, J.; Fazekas, F.; Filippi, M.; Freedman, M.S.; et al. Diagnosis of multiple sclerosis: 2017 revisions of the McDonald criteria. *Lancet Neurol.* **2018**, *17*, 162–173. [CrossRef] [PubMed]
30. Fisk, J.D.; Pontefract, A.; Ritvo, P.G.; Archibald, C.J.; Murray, T.J. The impact of fatigue on patients with multiple sclerosis. *Can. J. Neurol. Sci.* **1994**, *21*, 9–14. [CrossRef]
31. Branton, W.G.; Zhang, N.; Cohen, E.A.; Brew, B.J.; Gill, M.J.; Gelman, B.B.; Kong, L.; Power, C. Brain RNA profiling highlights multiple disease pathways in persons with HIV-associated neurocognitive disorder. *AIDS* **2025**, *39*, 496–507. [CrossRef] [PubMed]
32. Branton, W.G.; Fernandes, J.P.; Mohammadzadeh, N.; Doan, M.A.; Laman, J.D.; Gelman, B.B.; Fagrouch, Z.; Kondova, I.; Mooij, P.; Koopman, G.; et al. Microbial molecule ingress promotes neuroinflammation and brain CCR5 expression in persons with HIV-associated neurocognitive disorders. *Brain Behav. Immun.* **2023**, *107*, 110–123. [CrossRef] [PubMed]
33. Skoufos, G.; Kakoulidis, P.; Tastsoglou, S.; Zacharopoulou, E.; Kotsira, V.; Miliotis, M.; Mavromati, G.; Grigoriadis, D.; Zioga, M.; Velli, A.; et al. TarBase-v9.0 extends experimentally supported miRNA-gene interactions to cell-types and virally encoded miRNAs. *Nucleic Acids Res.* **2024**, *52*, D304–D310. [CrossRef] [PubMed]

Disclaimer/Publisher's Note: The statements, opinions and data contained in all publications are solely those of the individual author(s) and contributor(s) and not of MDPI and/or the editor(s). MDPI and/or the editor(s) disclaim responsibility for any injury to people or property resulting from any ideas, methods, instructions or products referred to in the content.